Transmemristance in multiterminal memristive nanowire networks

Transmemristance in multiterminal memristive nanowire networks

1st Gianluca Milano
Istituto Nazionale di Ricerca Metrologica (INRiM)
Strada delle Cacce 91, 10135 Torino, Italy
g.milano@inrim.it

2nd Alessandro Cultrera
Istituto Nazionale di Ricerca Metrologica (INRiM)
Strada delle Cacce 91, 10135 Torino, Italy
a.cultrera@inrim.it

3rd Enrique Miranda
Universitat Autònoma de Barcelona
08193 Cerdanyola del Valles, Spain
enrique.miranda@uab.cat

4th Carlo Ricciardi
Politecnico di Torino
C.so Duca degli Abruzzi 24, 10129 Torino
carlo.ricciardi@polito.it

***Abstract*— Memristive systems have been extensively explored for the realization of novel computing hardware architectures. In addition to conventional crossbar arrays based on two-terminal memristive cells, multiterminal memristive systems formed by self-organizing networks of nanoscale components have attracted growing interest. Here, we discuss the concept of *transmemristance* in multiterminal memristive networks, where emergent memristive behavior arises from the mutual interactions among a large number of nanowires (NWs). We show that transmemristance offers a new perspective for probing the internal dynamics of such systems, providing insights into their spatiotemporal evolution. Moreover, it can serve as a measurable physical quantity that reflects the internal state of the network and can be harnessed for the hardware implementation of unconventional computing paradigms.**

Keywords—multiterminal memristive systems, nanowire networks, transmemristance

I. Introduction

Nanowire (NW) networks have been reported as physical substrates for the implementation of unconventional computing paradigms, such as reservoir computing [1], [2]. These implementations rely on multiterminal configurations, where multiple electrodes enable external stimulation and/or readout of the spatiotemporal evolution of the system's internal state. In such multiterminal systems, the internal state can be described either by the system's conductance matrix, a matrix containing the effective conductance between any two terminals of the network, or by voltage maps, obtained by recording the floating voltage at terminals located in different regions of the network) [3]. Conductance matrices provide information about the effective network conductance as seen from the system terminals and are constructed through a sequence of measurements (i.e., the effective conductance cannot be measured simultaneously for multiple electrode pairs unless their spatial separation is sufficiently large). In contrast, voltage maps enable simultaneous probing of the system's internal state at multiple spatial locations during external voltage stimulation, but they provide only indirect information about the internal resistive state of the network. The possibility of simultaneously recording floating voltages at multiple locations via voltage mapping has been exploited to access the internal spatiotemporal evolution of NW networks for information processing, particularly in the context of reservoir computing [3], [4]. Furthermore, it has been demonstrated that the internal state of multiterminal NW networks can be retrieved through Electrical Resistance Tomography (ERT), a technique that reconstructs the conductance map of a multiterminal system via a sequence of transresistance measurements [5], [6]. The evolution of conductivity maps obtained by ERT has been used to experimentally monitor the spatiotemporal dynamics of multiterminal nanowire networks, including both short-term and long-term memory effects [7]. Here, we show that the dynamic evolution of transresistance in a multiterminal memristive system driven by external stimulation, i.e., the transmemristance, represents a measurable physical observable that conveys information about the local network activity, providing a new means to monitor the emergent dynamics of these systems from a different perspective.

Experimental results

A. Multiterminal memristive nanowire network

Memristive Ag nanowire (NW) networks can be fabricated by drop-casting NWs dispersed in solution onto an insulating substrate, as detailed in a previous work [8]. In this study, multiterminal NW networks were realized by drop-casting NWs onto a 1 × 1 cm quartz substrate, which was then mounted in a custom fixture where spring-loaded needle probes provided multiple electrical connections to the network (details in Ref. [5]). A conceptual schematic of the multiterminal NW network, featuring a switching matrix that enables reconfigurable wiring configurations, is shown in Fig. 1a. When stimulated between any two electrodes, the system exhibits an emergent (effective) memristive behavior arising from resistive switching effects at the NW junctions [8].

B. Transresistance matrix

At a given time t, the multiterminal network can be electrically described by the transresistance matrix of the system, where each off-diagonal element $T_{ij,kl}$ represents a transresistance that relates the current I^{src} flowing between terminals i and j with the voltage V^{sense} measured between terminals k and l (while keeping all other terminals floating).

G.M. acknowledges funding by the European Union (ERC, "MEMBRAIN", No. 101160604). A.C. acknowledges funding by the European Union under the Horizon Europe in the Framework of the EMPHASIS Project (https://www.emphasis-supercaps.eu/), Grant 101091997.

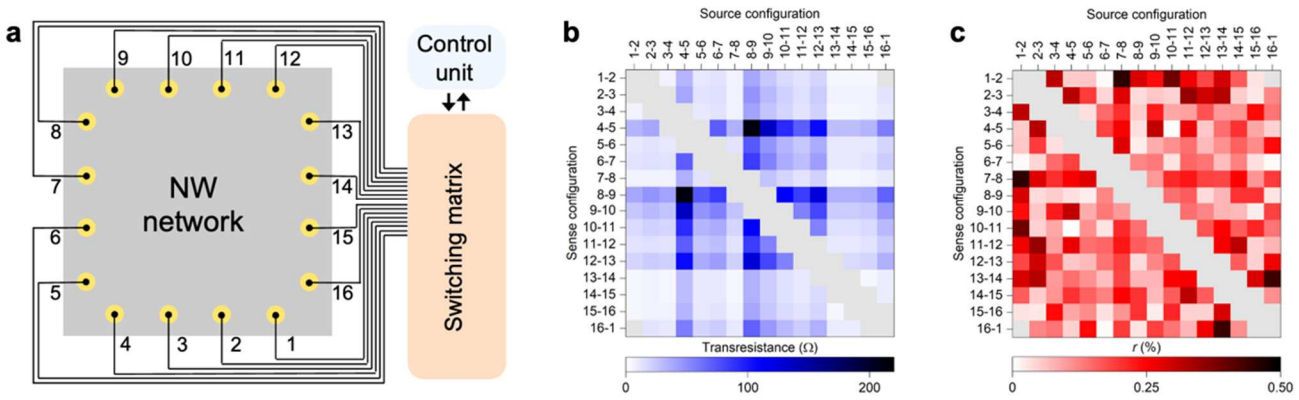

Fig. 1. a) Conceptual schematization of a multiterminal memristive NW network; b) Impedance matrix of the system where each element represents the transmemrsitace in between selected configurations (grey elements involving two-terminal and three-terminal measurements are not measured); c) reciprocity matrix where each element represents the reciprocity error (in percentage) of the corresponding transresistance measurement.

The transresistance between terminals ij and kl can thus be defined as:

$$T_{ij,kl} = V_{kl}^{sense}/I_{ij}^{src}$$

A constant-voltage protocol, consisting of measuring I_{ij}^{src} while sourcing a constant voltage $V_{ij}^{\mathrm{src}} = 10\ \mathrm{mV}$, was applied to obtain the transresistance matrix while avoiding sample alteration [6]. In our case, for multiterminal NW networks with $n = 16$ electrodes, the set of transresistances describing the system was acquired using the so-called adjacent measurement scheme, which involves $N = n \times (n-3) = 208$ transresistance measurements. These measurements are represented in the transresistance matrix shown in Fig. 1b. It should be noted that this matrix represents a portion of the full impedance matrix, since it includes only four-terminal measurements, in which the effect of contact resistances is excluded. In contrast, elements corresponding to two-terminal and three-terminal configurations, where contact resistance contributes, are not considered (grey elements in the matrix). The transresistance matrix, which differs from that of an electrically uniform 2D material, reflects the local electrical conductivity of the system and can be related, for instance, to local variations in NW network density. In this sense, the transresistance matrix conveys information about the spatial distribution of conductivity across the NW network device.

Figure 1c shows an evaluation of the reciprocity (in percentage) of the transresistance matrices, where each element is calculated as:

$$r_{ij,kl} = 2|(T_{ij,kl} - T_{kl,ij})/(T_{ij,kl} + T_{kl,ij})\,|$$

This quantity represents the deviation between reciprocal measurements with respect to their mean value. By employing the constant-voltage measurement protocol, low deviations (<0.5%) are typically observed as expected for a linear reciprocal network. The high reciprocity of the NW network is further corroborated by evaluating the asymmetry index of the matrix, as reported in Ref. [6]:

$$v = \|Z - Z^T\|_F / \|Z + Z^T\|_F$$

where Z^T is the transposed matrix, while F indicate the Frobenius norm. The value $v = 7 \times 10^{-4}$ obtained for the example shown in Fig. 1b reflects the high symmetry of the matrix ($v \to 0$ for a perfectly symmetric matrix). This high degree of symmetry not only confirms that the network is reciprocal but also indicates that the transresistance measurements themselves do not alter the sample.

C. *Memristance and transmemristance*

In multiterminal memristive systems, where the internal resistive state evolves over time in response to external electrical stimulation, the temporal evolution of transresistance, i.e., the *transmemristance*, provides information about the spatiotemporal dynamics of the system.

Figure 3a shows the evolution of the effective conductance between pairs of electrodes that were sequentially stimulated with a voltage pulse (2 V, 5 s). Here, the conductance time traces arise from the two-terminal effective memristive behavior of the system, as observed from the specific pair of terminals used for stimulation.

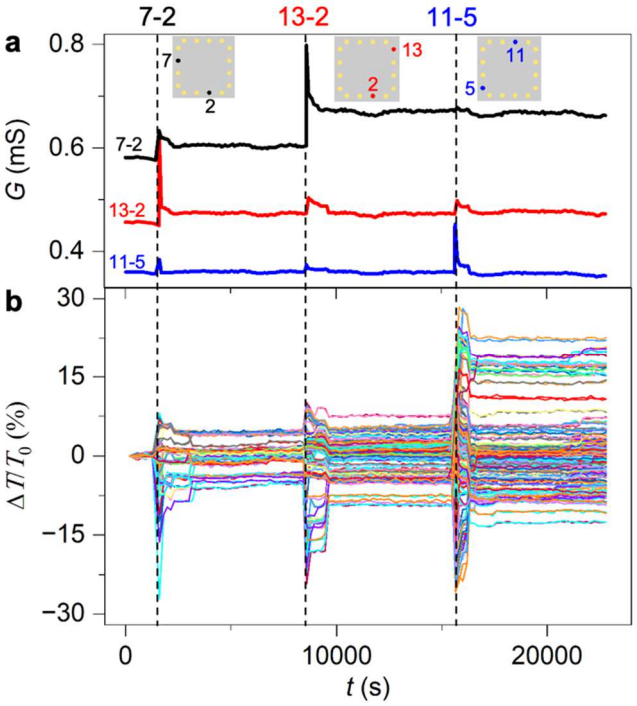

Fig. 2. a) Conductance time traces of selected terminal pairs sequentially stimulated in different configurations with a voltage pulse (2V, 5s). The inset reports the specific configuration stimulated in correspondance with the dashed line. b) Evolution of transconductance curves (all 208 configurations) in terms of percentage changes with respect to the pristine transconductance.

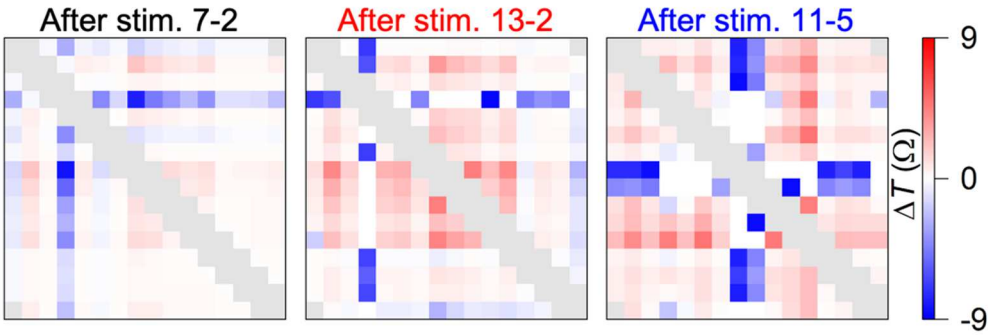

Fig. 3. Evolution of transresistance matrices in terms of variations with respect to the pristine state tranresistance matrix. Each differential transresistance matrix reflects the evolution of the system immediately after the end of a specific stimulation during the stimulation sequence reported in Fig. 2a.

It can be observed that both short-term memory effects (a progressive spontaneous decrease of the effective conductance after stimulation) and long-term memory effects are present. While short-term memory effects are associated with volatile resistive switching in NW junctions, long-term ones are attributed to more persistent reconfigurations of the NW network [7]. As can be seen, the stimulation of a specific pair of electrodes also induces changes in the effective conductance between other, unstimulated electrode pairs. This behavior was shown to emulate heterosynaptic plasticity effects typical of biological networks [8]. The intensity of conductance changes at non-stimulated terminals depends on both the network topology and the spatial position of the terminals. In the example of Fig. 2a, the stimulation of terminals 7–2 leads to more pronounced changes in the effective conductance between terminals 13–2 (which share a common electrode) compared to terminals 5–11. Figure 2b shows the corresponding evolution of transmemristances measured across all 208 possible four-terminal configurations. Markedly different dynamics, in both sign and magnitude, are observed across different configurations. This occurs because transmemristance dynamics depend on the spatial relationship between the source and sense terminals in a given configuration, as well as on the properties and location of the conductive pathways formed between the stimulated electrodes. Importantly, the transmemristance dynamics (Fig. 2b) may differ in their characteristic timescales from the memristive dynamics observed at the stimulating electrodes (Fig. 2a). In the reported example, the relaxation timescale of short-term memory effects in some transmemristance curves is larger than the relaxation timescale of memristive timetraces. Thus, certain regions of the network may continue to evolve dynamically even when no variations are detected in the two-terminal memristive response. In other words, the local memristive activity is not necessarily reflected in the effective behavior measured between the two terminals.

The local memristive activity of the network can be deepened by examining the transresistance matrices after each stimulation. Figure 3c shows the differential transresistance matrices calculated with respect to the pristine-state matrix (i.e., before stimulation) for each stimulated pair of terminals. As can be seen, the largest variations in transresistance are localized between pairs of terminals that are spatially located in specific regions of the network, reflecting the distinctive reconfiguration of the network following electrical stimulation. Transresistance matrices can be exploited as input data for spatially resolved conductivity mapping of NW networks via electrical resistance tomography (ERT) [7]. However, ERT map reconstruction involves solving an ill-posed inverse problem, which is inherently sensitive to measurement noise and fluctuations in the measured physical quantities. In practical cases where ERT reconstruction may fail for specific samples, the transmemristance and transresistance matrices themselves still provide valuable insights into the local activity and spatiotemporal memristive behavior of the system.

II. Conclusions

In summary, we show that the dynamics of multiterminal memristive NW networks can be effectively analyzed through transmemristance. This quantity enables probing of internal states, characterization of dynamic behavior, and functional access to memory states—capabilities relevant to unconventional computing applications.

References

[1] G. Milano, K. Montano, and C. Ricciardi, ‘In materia implementation strategies of physical reservoir computing with memristive nanonetworks’, *J Phys D Appl Phys*, vol. 56, no. 8, p. 084005, Feb. 2023, doi: 10.1088/1361-6463/acb7ff.

[2] G. Milano *et al.*, ‘In materia reservoir computing with a fully memristive architecture based on self-organizing nanowire networks’, *Nat Mater*, vol. 21, no. 2, pp. 195–202, Feb. 2022, doi: 10.1038/s41563-021-01099-9.

[3] D. Pilati, F. Michieletti, A. Cultrera, C. Ricciardi, and G. Milano, ‘Emerging Spatiotemporal Dynamics in Multiterminal Neuromorphic Nanowire Networks Through Conductance Matrices and Voltage Maps’, *Adv Electron Mater*, Nov. 2024, doi: 10.1002/aelm.202400750.

[4] F. Michieletti, D. Pilati, G. Milano, and C. Ricciardi, ‘Self-organized Criticality in Neuromorphic Nanowire Networks With Tunable and Local Dynamics’, *Adv Funct Mater*, 2025, doi: 10.1002/adfm.202423903.

[5] G. Milano *et al.*, ‘Mapping Time-Dependent Conductivity of Metallic Nanowire Networks by Electrical Resistance Tomography toward Transparent Conductive Materials’, *ACS Appl Nano Mater*, p. acsanm.0c02204, Oct. 2020, doi: 10.1021/acsanm.0c02204.

[6] A. Cultrera, G. Milano, N. De Leo, C. Ricciardi, L. Boarino, and L. Callegaro, ‘Recommended implementation of electrical resistance tomography for conductivity mapping of metallic nanowire networks using voltage excitation’, *Sci Rep*, vol. 11, no. 1, p. 13167, Dec. 2021, doi: 10.1038/s41598-021-92208-w.

[7] G. Milano, A. Cultrera, L. Boarino, L. Callegaro, and C. Ricciardi, ‘Tomography of memory engrams in self-organizing nanowire connectomes’, *Nat Commun*, vol. 14, no. 1, p. 5723, Sep. 2023, doi: 10.1038/s41467-023-40939-x.

[8] G. Milano *et al.*, ‘Brain-Inspired Structural Plasticity through Reweighting and Rewiring in Multi-Terminal Self-Organizing Memristive Nanowire Networks’, *Advanced Intelligent Systems*, vol. 2, no. 8, p. 2000096, Aug. 2020, doi: 10.1002/aisy.202000096.